

# A Finite Element Model for Simulating Flow around a Well with Helically Symmetric Perforations

S. Amirodin Sadrnejad<sup>1</sup>, Hasan Ghasemzadeh<sup>2</sup>,  
AhmadAli Khodaei Ardabili<sup>\*3</sup>

1, 2, 3. Faculty of Civil Engineering, K. N. Toosi University of  
Technology, Tehran, Iran

Received: 8 May 2017

Revised: 8 July 2017

## Abstract

In a perforated well, fluids enter the wellbore through arrays of perforation tunnels. These perforations are typically distributed in a helical pattern around the wellbore. Available numerical models to simulate production flow into cased-and-perforated vertical wells have complicated boundary conditions or suffer from high computational costs. This paper presents a simple and at the same time efficient finite element model to simulate flow around a well with helically symmetric perforations. In the proposed model, by taking advantage of the symmetry, only a thickness of perforated interval containing a single perforation tunnel needs to be meshed. Angular phasing between adjacent perforations is considered by applying periodic boundary conditions on the upper and lower boundaries of the representative reservoir thickness. These boundary conditions involve periodic-pressure and periodic-velocity parts. Unlike the periodic-pressure part, the method of imposing the periodic-velocity condition

---

Corresponding author: khodaie@dena.kntu.ac.ir

within a single-variable flow problem is rather vague. In this regard, it is proved that in the proposed model, periodic-velocity condition is automatically satisfied in a weak sense. The accuracy and the computational efficiency of the proposed model are verified through comparison with available models. The model results, in terms of skin factor, are compared with the common semi-analytical model as well, and good agreement is obtained. The proposed model can readily be used as a numerical tool to study inflow of wells with helically symmetric perforations.

**Keywords:** Cased and perforated well, Finite element method, Helical symmetry, Periodic boundary condition, Well inflow analysis.

## Introduction

Cased and perforated completion is one of the most widely used well completion techniques all around the world [1], [2]. In a perforated well, fluids enter the wellbore through an array of perforations, which have penetrated into the casing, cement sheath and a certain depth of reservoir [3]. The perforations are commonly created by shaped charge jet perforators [4] and have the form of helically distributed tunnels around the wellbore [5]. Angle between two successive perforations (phasing) is commonly selected to be 0, 180, 90 and 60 degree [6]. The density of the perforations may vary from 6 to 52 shots per meter (SPM) of the wellbore length [2]. Figure 1 shows some perforating guns with helically distributed shaped charges.



**Figure 1. Loading shaped charges into perforating guns [6]**

An accurate prediction of flow field from the producing reservoir to the perforated well is of a great significance for conducting well performance optimization processes. Prediction of flow variables in the vicinity of the perforations is also vital to sand production analyses. However, fluid flow into perforated completions has a complex three-dimensional (3D) convergent pattern. On the other hand, because of the helical arrangement of the perforations, simple no-flow boundaries between adjacent perforations cannot be distinguished in general. Analytical treatment of such a flow pattern is extremely difficult [5] and numerous simplifying assumptions are required to handle this problem. Nevertheless, numerical methods and especially finite element method (FEM) provide a versatile tool to simulate flow around perforations.

Various numerical models have been developed to study steady-state inflow of perforated wells. Harris (1966) [7] published the first

numerical simulation of the perforated completions. In his finite difference model, perforations were assumed to be wedge shaped and in the same horizontal plane. Klotz et al. (1974) [8] were the first to apply the FEM to this problem. However, their model was two-dimensional. Locke (1981) [9] considered a variety of realistic perforating parameters and used a commercial finite element software to simulate the flow around perforated wells. He modeled half of a horizontal section containing one perforation and extending halfway up and down to the adjoining perforations. Angular phasing was achieved by a complicated coupling of boundary nodes together. Dogulu (1998) [10] developed an extremely CPU intensive approach with full modeling of the perforating interval to estimate productivity of a well. Ansah et al. (2002) [11] applied a commercial finite element code to develop a new wellbore inflow model in which a cone-shaped perforation geometry with a tapered tip was incorporated. They explicitly modeled eighteen perforation tunnels in their representative reservoir thickness. Jamiolahmady et al. (2007) [12] developed a 3D finite element flow simulator to investigate gas-condensate flow around long perforations. They did not define any boundary condition for top and bottom sides of their perforated well model, which are equivalent to the no-flow boundaries in the standard FEM. Byrne et al. (2009) [13] employed a computational fluid dynamics (CFD) software to predict well performance, based on high quality laboratory testing. Their analyses were two-dimensional and angular phasing was not

considered. Sun et al. (2013) [14] used a commercial CFD software to investigate flow characteristics around the perforated wells. Their representative 3D geometric formation contains one cycle of perforation tunnels. Periodic top and bottom boundary conditions were applied to simulate infinite thickness of the formation. Volonte et al. (2013) [15] and Wang et al. (2016) [16], as many other researchers, assumed that each cycle of the perforations is in the same horizontal plane.

Most of the above-mentioned models have incorporated repeating patterns of the flow in order to restrict the computational domain to a small part of the formation. However, they are not efficient enough or have unrealistic or complicated boundary conditions.

Imposing the periodic boundary conditions in the CFD analyses is a well-established issue. For example, Segal et al. (1994) [17] described implementation of the periodic boundary conditions for flows governed by incompressible Navier-Stokes equations. However, to the best of the authors' knowledge, in the context of finite element solution of single variable seepage problem, there is no explicit account available about the enforcement of the periodic boundary conditions. It is worth noting that Li (2012) [18] concerning with micromechanical finite element analysis, proved that the periodic traction boundary conditions are natural boundary conditions from the minimum total potential energy principle.

The main objective of this paper is to propose a simple and at the same time, accurate finite element model for simulating the flow into perforated wells. In this regard, repetitive nature of the flow geometry is employed to select an appropriate representative geometric formation to achieve a balance between the simplicity and the computational efficiency. It is also proved that periodic-velocity condition is automatically satisfied on the model boundaries.

### **Symmetry of the flow pattern around the perforated wells**

Figure 1 shows a schematic view of a perforated completion with a spiral distribution of perforations. This figure depicts two cycles of perforation tunnels with angular phasing of 120 degrees. Drilling damage zone around the wellbore and crushed zone around the perforation tunnels are also depicted in this figure. Flow geometry at the drainage radius of the well, could be considered radial; however, it resembles a complex three-dimensional convergent pattern near the wellbore.

In many practical cases, numerous perforations are generated in the reservoir pay zone (Figure 1). Because of the spiral arrangement of the perforations, simple no-flow boundaries between adjacent perforations cannot be utilized to restrict the computational domain to a manageable size [19]. Therefore, numerical simulations of such a

problem, considering the whole geometry, are commonly very time consuming or impossible.

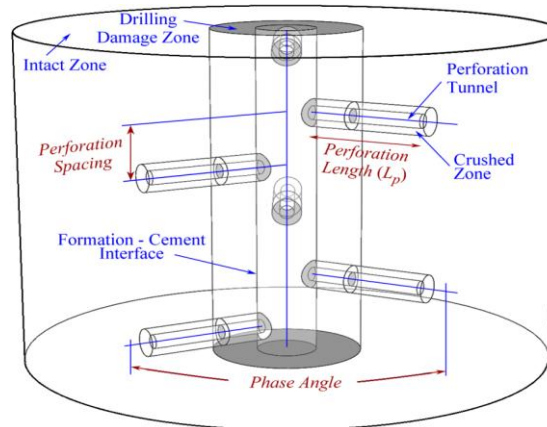


**Figure 2. Schematic view of a perforated well with 120° phasing**

Fortunately, in most cases, the solution of the flow problem is expected to reproduce some types of repeating patterns. Taking advantage of these patterns, one can efficiently model a small part of the geometry. Figure 3 presents iso-pressure surfaces for two cycles of a virtually infinite system of perforations. In this figure, two types of repetition, between each cycle of perforations and each perforation can readily be distinguished. In addition, considering each individual perforation, a rotational type of symmetry with respect to the perforation axis can be recognized.

Conditions required for the repetitive flow pattern to form around a perforated well can be summarized as:

- Perforated interval has to be long enough and cover all the pay zone thickness to ignore end effects.

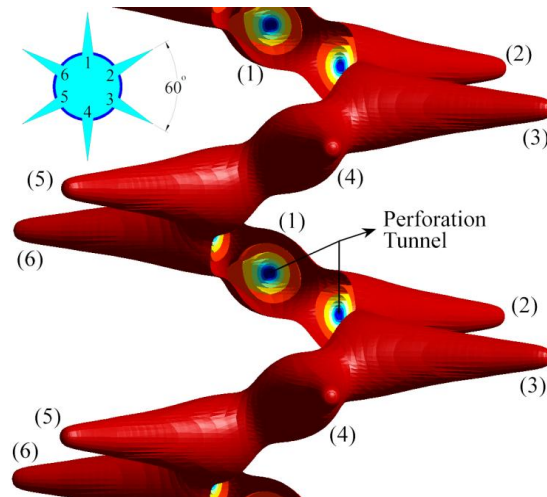


**Figure 3. Typical iso-pressure surfaces around a perforated well with 60° phasing**

- A repeating pattern in geometry has to be distinguishable between perforation tunnels and also between crushed zones.
- A repeating pattern in material properties is to exist between any two perforation layers. Considering permeability tensor, this requires one of the principal directions coincides with the wellbore axis and the two other principal values to be equal.
- Formation inlet pressure and bottom-hole flowing pressure have to be uniform along the wellbore

When all the above conditions are met, it is possible to consider only a small representative part of the formation for analysis. In this respect, appropriate periodic boundary conditions must be applied to the representative unit in order to reproduce the expected pattern of symmetry.



### Available numerical models

Available numerical models for the perforated wells that utilize the symmetric flow patterns can be categorized in the following two groups:

One-cycle models (OCM): in this category of models using translational symmetry, perforations in one screw pitch of the perforated interval are simulated (Figure 4). Each node on the bottom boundary with coordinates  $(x_i, y_i, z_i)$  must be coupled with a node located in  $(x_i, y_i, z_i + (360/\phi) h)$ , where  $h$  is the perforation spacing and  $\phi$  is the angular phasing between two successive shots. Sun et al. (2013) [14] first reported and used this model.

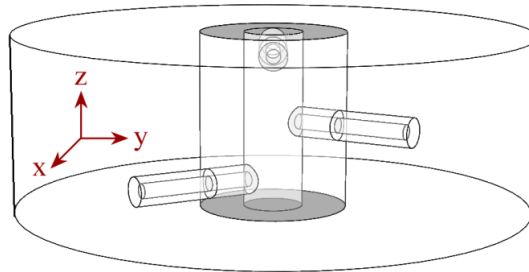


**Figure 4. Typical computational domain of a one-cycle model (OCM) for angular phasing of 120°**

Half-perforation models (HPM): taking full advantage of helically and rotational symmetries, this model category just requires one-half of a perforation layer to be explicitly simulated (Figure 5). In this model which proposed by Lock (1981), coupling nodes are located on the both horizontal and vertical boundaries of the model. It is not a trivial task to identify these nodes. Moreover, different node sets must be defined for different phasing angles. For example, coupled nodes on the wellbore surface for 90° phasing is illustrated in Figure 6.

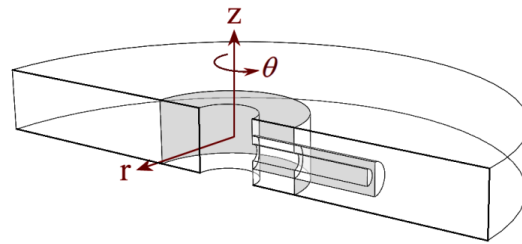


**Figure 5. Typical computational domain of a half-perforation model (HPM)**

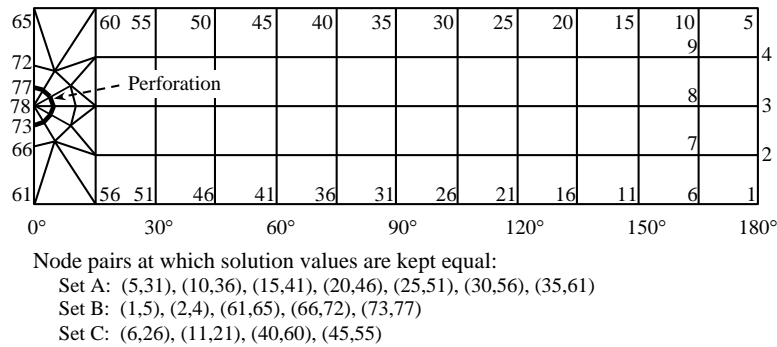


**Figure 6. Node specification and coupled sets of nodal values for 90° phasing on the wellbore surface with coarse elements**

Simplicity of the boundary conditions is the main advantage of the one-cycle model category. However, it is time consuming and costly to conduct a simulation with this model, especially for completions with small phasing angles. Half-perforation model is an ultra-high efficient one. Nevertheless, it suffers from complexity of the boundary conditions. This may be the reason why application of this approach has not been reported during the past two decades.

### Details of the proposed model

In the petroleum industry, numerical simulation of flow into perforated completions can be a useful tool for optimizing well

productivity and designing more economic completions. In this regard, it is neither efficient nor required, in most cases, to simulate full length of the perforated interval. However, available models which allow considering a representative unit have complicated boundary conditions or suffer from higher computational costs.

The proposed model in this study has simple boundary conditions and is efficient enough to be used as a numerical tool for modeling inflow of cased-and-perforated vertical wells.

### 1. Model Assumptions

The main assumption in the developed model is the existence of a helically symmetric pattern around the wellbore. Prerequisites for the validity of this assumption are repetitive symmetry of geometry, material properties and boundary conditions in a helical manner. The problem with this type of symmetry can be efficiently solved over a small representative unit; provided that appropriate periodic boundary conditions are imposed.

The computational domain of the model with the basic notation is illustrated in Figure 7. In this figure,  $h$  is the spacing between two successive perforations,  $L_p$  and  $r_p$  are the perforation length and radius,  $r_w$  and  $r_e$  are the wellbore and drainage radius, and  $r_d$  and  $r_c$  are the drilling damage and crushed zone radius, respectively. As shown in Figure 7, a horizontal section of the formation containing one perforation tunnel needs to be analyzed. Currently cylindrical shaped perforation is included; however, it is possible to use more realistic cone-shaped perforations.

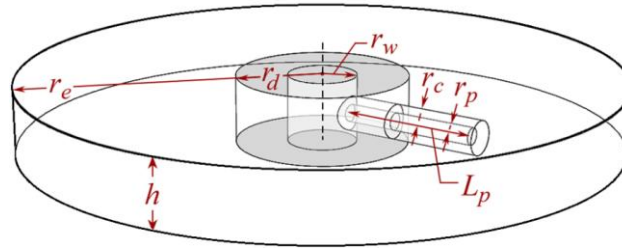


**Figure 7. Representative geometric formation of the proposed model**

For the sake of simplicity, the steady state flow of an incompressible single phase fluid is investigated in this paper. Moreover, gravity effects were ignored and it is assumed that Darcy law is valid.

With these assumptions, the governing equation of the model can be written as Laplace's equation:

$$-\frac{1}{\mu} \left( \kappa_x \frac{\partial^2 p}{\partial x^2} + \kappa_y \frac{\partial^2 p}{\partial y^2} + \kappa_z \frac{\partial^2 p}{\partial z^2} \right) = 0 \quad (1)$$

where  $p$  is fluid pressure,  $\kappa_x$ ,  $\kappa_y$  and  $\kappa_z$  are the principal permeability in the  $x$ ,  $y$  and  $z$  directions, respectively, and  $\mu$  is the fluid viscosity.

## 2. Boundary conditions

A System with repetitive symmetry can be characterized as a periodical array of representative units. Applying appropriate periodic boundary conditions on a representative unit ensures continuity of the variables on the boundaries [20, 21].

In the proposed model each node on the bottom boundary with cylindrical coordinates  $(r_i, \theta_i, z_i)$  must be coupled with a node located in  $(r_i, \theta_i + \phi, z_i + h)$ . In the finite element solution of the single variable seepage problem in porous media with repetitive symmetry,

these periodic boundary conditions must ensure repeating of pressure and velocity fields on the opposite sides of the representative unit.

Using the standard FEM, equivalent weighted-integral form of (1) is obtained as:

$$\begin{aligned} & \frac{1}{\mu} \int_{\Omega} \left[ \kappa_x \frac{\partial w}{\partial x} \frac{\partial p}{\partial x} + \kappa_y \frac{\partial w}{\partial y} \frac{\partial p}{\partial y} + \kappa_z \frac{\partial w}{\partial z} \frac{\partial p}{\partial z} \right] dx dy dz \\ & - \frac{1}{\mu} \oint_{\Gamma} w \left( \kappa_x \frac{\partial p}{\partial x} n_x + \kappa_y \frac{\partial p}{\partial y} n_y + \kappa_z \frac{\partial p}{\partial z} n_z \right) ds = 0 \end{aligned} \quad (2)$$

in which,  $w$  is the weight function,  $\Gamma$  is the domain boundary,  $n_x$ ,  $n_y$  and  $n_z$  are components of the unit normal vector on the boundary, and  $ds$  is the area of an infinitesimal surface element on the boundary.

If  $\Gamma^+$  and  $\Gamma^-$  are two opposite parts of the boundary  $\Gamma$ , which are related by helical symmetry in a piecewise manner, periodic boundary conditions to be imposed are:

$$p|_{\Gamma^+} = p|_{\Gamma^-} \quad (3)$$

$$\{v_x, v_y, v_z\}|_{\Gamma^+} = \{v_x, v_y, v_z\}|_{\Gamma^-} \quad (4)$$

where  $v_x$ ,  $v_y$  and  $v_z$  are components of superficial velocity vector, and can be derived from post processing of the solution.

In Equation (2),  $p$  is the primary variable and its specification on the boundary constitutes the essential boundary condition ([22]). Therefore, enforcement of (3), which is periodic-pressure part of the boundary conditions, is straightforward and can be achieved as multi-point constraints (MPC) equations ([23]). In this respect, it is required that the pressure of each node with cylindrical coordinates of  $(r_i, \theta_i, z_i)$  on the lower boundary be kept equal with the pressure of a node with coordinates of  $(r_i, \theta_i + \phi, z_i + h)$  on the upper boundary.

Constraint Equation (4) is the velocity-periodic part of the boundary conditions. In the context of the finite element solution of the single variable seepage problem, there is no explicit account available about the imposing of the velocity-periodic part. It is the objective of this section to address this ambiguity.

The boundary integral in (2) contributing to the  $\Gamma^+$  and  $\Gamma^-$  can be expanded as below.

$$\int_{\Gamma^+ \cup \Gamma^-} w \left( \kappa_x \frac{\partial P}{\partial x} n_x + \kappa_y \frac{\partial P}{\partial y} n_y + \kappa_z \frac{\partial P}{\partial z} n_z \right) ds = \int_{\Gamma^+} w \left( \kappa_x \frac{\partial P}{\partial x} n_x + \kappa_y \frac{\partial P}{\partial y} n_y + \kappa_z \frac{\partial P}{\partial z} n_z \right) ds + \int_{\Gamma^-} w \left( \kappa_x \frac{\partial P}{\partial x} n_x + \kappa_y \frac{\partial P}{\partial y} n_y + \kappa_z \frac{\partial P}{\partial z} n_z \right) ds \quad (5)$$

Applying Darcy law to the velocity-periodic part (i.e. (4)), yields to:

$$\left\{ \kappa_x \frac{\partial p}{\partial x}, \kappa_y \frac{\partial p}{\partial y}, \kappa_z \frac{\partial p}{\partial z} \right\} \Big|_{\Gamma^+} = \left\{ \kappa_x \frac{\partial p}{\partial x}, \kappa_y \frac{\partial p}{\partial y}, \kappa_z \frac{\partial p}{\partial z} \right\} \Big|_{\Gamma^-} \quad (6)$$

On the other hand if  $\Gamma^+$  and  $\Gamma^-$  be parallel to each other and equal in shape, which is the case considering repetitive symmetry, following equations can readily be obtained:

$$\{n_x, n_y, n_z\} \Big|_{\Gamma^+} = -\{n_x, n_y, n_z\} \Big|_{\Gamma^-} \quad (7)$$

$$\int_{\Gamma^+} w ds = \int_{\Gamma^-} w ds \quad (8)$$

Using (6) and (7), we can write (8) as follows:

$$\int_{\Gamma^+} w \left( \kappa_x \frac{\partial P}{\partial x} n_x + \kappa_y \frac{\partial P}{\partial y} n_y + \kappa_z \frac{\partial P}{\partial z} n_z \right) ds = - \int_{\Gamma^-} w \left( \kappa_x \frac{\partial P}{\partial x} n_x + \kappa_y \frac{\partial P}{\partial y} n_y + \kappa_z \frac{\partial P}{\partial z} n_z \right) ds \quad (9)$$

Substituting of (9) into (5) vanishes boundary integrals over  $\Gamma^+$  and  $\Gamma^-$  which are periodic boundary surfaces. This means that for the proposed model the periodic-velocity part of the boundary conditions is automatically satisfied in a weighted integral sense and no treatment is required.

Essential boundary conditions involve prescribed pressure value on the outer boundary,  $p_e$ , and prescribed pressure value on the surface of the perforation tunnel,  $p_w$ . Wellbore surface is a no-flow boundary and consequently does not need any treatment. Boundary conditions of the model are depicted in Figure 8.

### 3. Meshing Strategy

Meshing of the upper and lower boundary surfaces must be satisfied in a manner that permits respective routine to detect paired nodes. In this regard, it is preferable that a mesh of circular and radial lines is used to discretize the top and bottom faces. However, other methods for imposing these types of conditions exist which can be used on arbitrary meshes (e.g. [24, 25]). A typical meshed geometry of the model is shown in Figure 9. In the current study, linear hexahedral elements with eight integration points are used to decompose the calculation domain. Because of large pressure gradients around the perforation tunnel, finer mesh is required in the respective zone. Details about assembly of element equations, determination of the shape functions and numerical integration can be found in books on the FEM such as [22, 23].

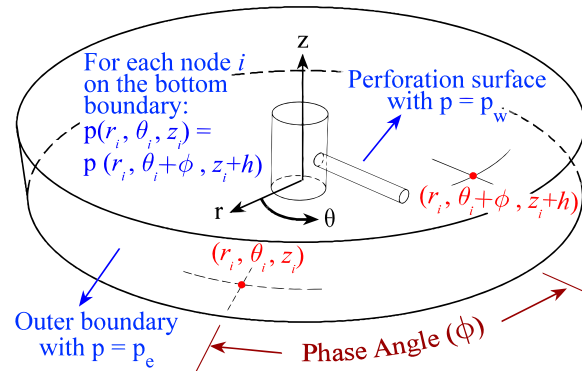


**Figure 8. Boundary conditions of the proposed model**

### Validation of the model

The proposed model contains only one perforation tunnel and reproduces a virtually infinite perforated interval. In order to demonstrate accuracy of the model, its results are compared against those for a model contains three cycles of perforations. Upper and lower boundaries of the three cycle model are assumed to be impervious. However, for a middle perforation with enough distances from the boundaries, results can be compared with the proposed model.

A perforated completion with shot density of 20 SPM (6 SPF) and angular phasing  $60^\circ$  is considered. Other input data are shown in Table 1. For this configuration, three cycle model contains eighteen perforations and a formation thickness of 0.9144 m (36 in) should be considered (corresponding to the values required for three perforation skew pitch). However, the proposed model contains only one perforation and formation thickness of 0.0508 m (2 in) is required to be modeled. Details of meshing for the three cycles of perforations are



shown in Figure 10. In the both models, the same number of elements were used to discretize each perforation layer.

Figures 11 and 12 show pressure and velocity values obtained on two horizontal circular paths with radius of  $r_w$  and  $r_w + L_p$ . For three cycle model, this horizontal circle belongs to the ninth perforation from bottom (see Figure 10 (c)). In these figures, angles are measured from axis of the perforation. Comparison of the results between these two models shows a reasonable coincidence, indicating accuracy of the proposed model for pressure and velocity estimations.

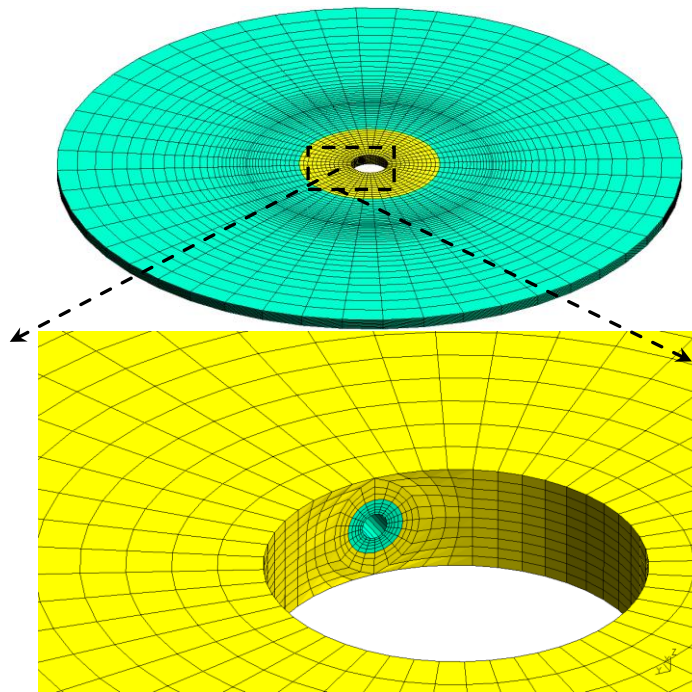


**Figure 9. Typical meshing for the proposed model**

**Table 1. Input data for model validation**

Parameter	Values
Well drainage radius ( $r_e$ )	1.524 m (60 in)
Wellbore radius ( $r_w$ )	0.0889 m (3.5 in)
Perforation length ( $L_p$ )	0.254 m (10 in)
Perforation tunnel radius ( $r_p$ )	0.00635 m (0.25 in)
Formation permeability ( $\kappa$ )	100 md ( $9.8692 \times 10^{-14} \text{ m}^2$ )
Fluid viscosity ( $\mu$ )	0.001 Pa.s (1 cp)
Pressure at external boundary ( $p_e$ )	1378.95 kPa (200 psig)
Pressure inside wellbore ( $p_w$ )	0 Pa (0 psig)

Unwrapped contour of pressure on the wellbore surface for the three-cycle model and the proposed model are shown in Figures 13 and 14, respectively. In these figures, a repetitive pattern of pressure contours around the innermost perforation and capability of the proposed model to reproduce this pattern using a smaller representative formation are evident

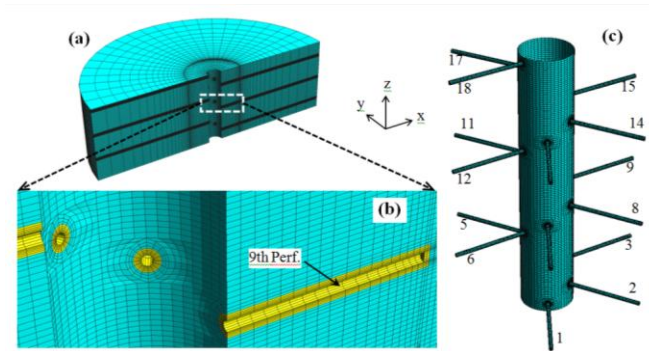


**Figure 10. Finite element meshes showing a 0.9144 m (3 ft) section with 20 SPM (6 SPF) and 60° phasing, a) Vertical section of the computational domain, b) details of the meshing near the wellbore, c) distribution of perforations around the wellbore**

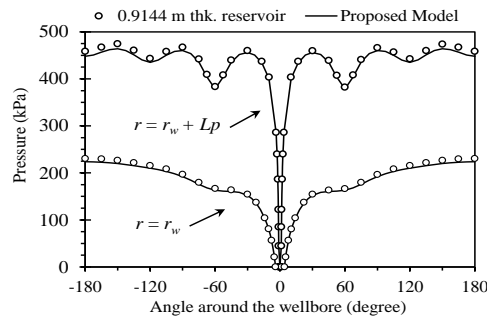


**Figure 11. Comparison of pressure between three-cycle model and the proposed model**

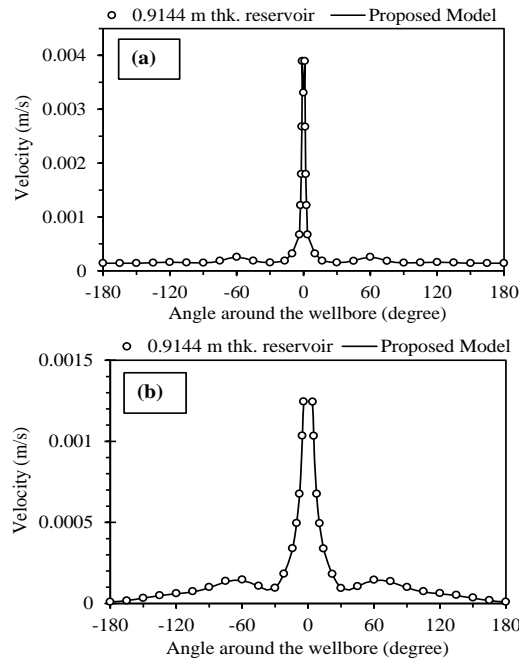


**Figure 12. Comparison of velocity between three-cycle model and the proposed model on a circular path with radius of: (a)  $r_w$  and (b)  $r_w + L_p$**

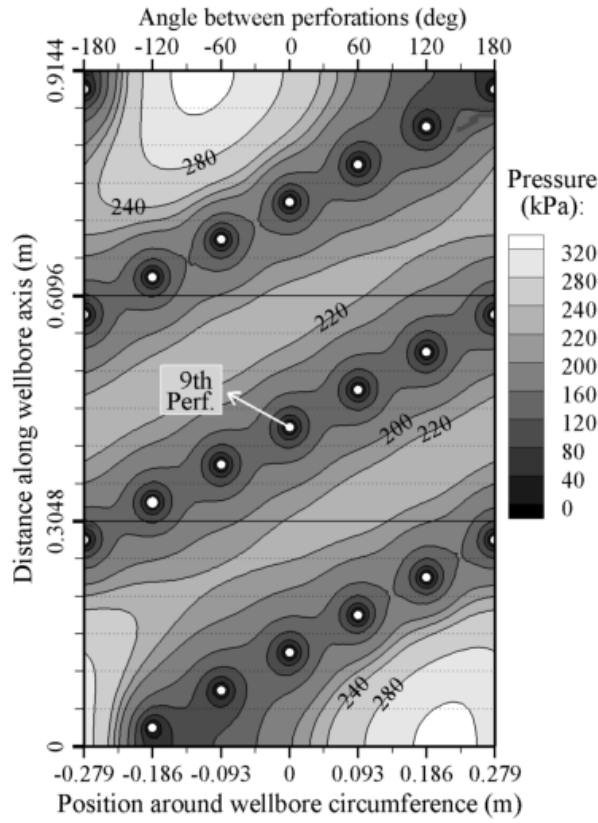


**Figure 13. Unrolled contour of pressure on cement-formation interface for three-cycle model**

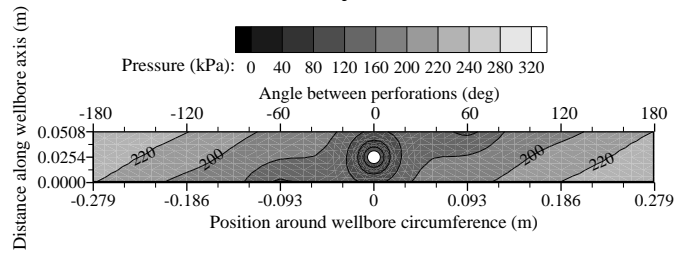


**Figure 14. Unrolled contour of pressure on cement-formation interface for the proposed model**

### Efficiency of the model

In order to examine computational efficiency of the proposed model, for some typical problems its CPU time were compared with those of one-cycle and half-perforation models. In this regard, three different configurations were considered: ( $n_s = 13$  SPM,  $\phi = 90^\circ$ ), ( $n_s = 20$  SPM,  $\phi = 60^\circ$ ) and ( $n_s = 26$  SPM,  $\phi = 45^\circ$ ). Other input data are the same as listed in Table 1. In each case, the proposed model comprises 58,401 degrees-of-freedom (DOFs). The same mesh densities were used for each perforation layer in the two other models.

Figure 15 shows normalized CPU time spent in simulation each pair of perforation density and phasing. This normalization is done through dividing calculated CPU time by that for the proposed model with  $n_s = 13$  SPM,  $\phi = 90^\circ$ . As shown in Figure 15, the proposed model is significantly more efficient than OCM. This efficiency increases dramatically with increasing the number of perforations tunnels in one skew pitch. In each case, HPM requires about half of the CPU time with respect to the proposed model. On the contrary, preparing boundary conditions of the HPM is more time consuming. Given that the total computational time of the proposed model is only a fraction of a minute, therefore it can be efficiently used in the analysis of perforated wells inflow.

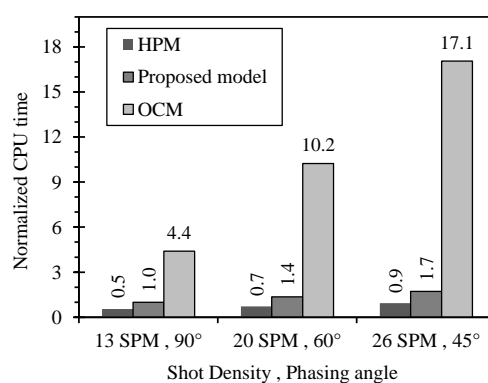


**Figure 15. Comparison of normalized CPU time between different models**

### Application to estimate skin factor

This section presents some verification examples to demonstrate the usefulness of the proposed numerical model in estimation of skin factor for perforated completions. In this regard, skin factors for some different configuration are computed and compared with the corresponding values from common semi-analytical Karakas-Tariq model ([5]).

Parameters range covered in this analysis are shown in Table 2. Fluid and formation properties are the same as given in Table 1. Permeability anisotropy and damaged zones around wellbore and perforation tunnels are not considered. These arise from some criticisms about the lack of generality for Karakas-Tariq model dealing with these cases (e.g. [10, 14, 26, 27, 28]).

Having the prediction of the flow rate, the skin factor,  $s$ , can be calculated as [29]:

$$s = \frac{2\pi \kappa h (p_e - p_w)}{q_p \mu} - \ln \left( \frac{r_e}{r_w} \right) \quad (10)$$

where  $q_p$  is flow rate from each perforation,  $\kappa$  is formation horizontal permeability, and  $r_w$  is the radius from the wellbore axis to the formation-cement interface.

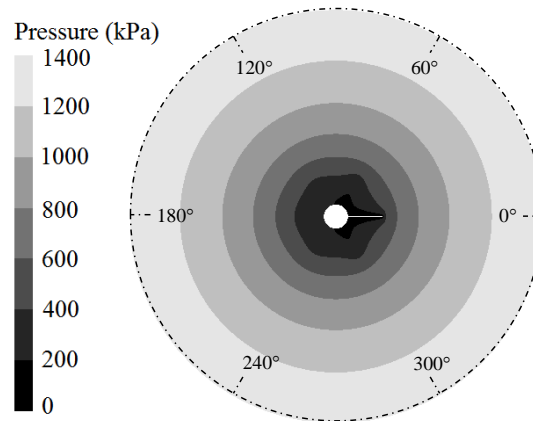
Before conducting the simulation, it is required to perform two sensitivity analyses; one for outer radius of the model to ensure radial flow at the far-field, and the other for mesh size to ascertain the effect of grid size on the results. Based on the first analysis, the reservoir outer size of 1.54 m (60 in) is enough to ensure less than 1% error in the solution. Based on the mesh sensitivity analysis, the mesh size was selected to ascertain less than 1% error in the results.

Figure 16 shows sample contour plot of pressure at a horizontal plane crossing the perforation axis. In this figure, radial flow pattern at the far-field and its convergence to the six perforations are obvious. Figure 17 depicts a predicted streamline pattern for a case with angular phasing of 60°. In this figure, the fluid flow across the periodic boundaries and its convergence to the adjacent perforations are evident.

Figure 18 demonstrates the comparison between the skin factor calculated from the proposed numerical model and the skin factor from the common semi-analytical model. This figure shows a good agreement between these models; however, there are small differences, which have also been reported by Sun et al. (2013) [14].

**Table 2. The range of parameters covered for skin factor calculations**

Parameter	Values
Shot density ( $n_s$ )	13 SPM (4 SPF) 20 SPM (6 SPF)
Phasing angle ( $\theta$ )	60° (for $n_s = 13$ SPM) 90° (for $n_s = 13$ and 20 SPM)
Wellbore radius ( $r_w$ )	0.0889 m (3.5 in)
Well drainage radius ( $r_e$ )	1.524 m (60 in)
Perforation length ( $L_p$ )	0.127 m (5 in) 0.254 m (10 in) 0.508 m (20 in)
Perforation radius ( $r_p$ )	0.00254 m (0.1 in) 0.00635 m (0.25 in)

**Figure 16. Pressure contours at the horizontal plane, crossing the perforation axis**

( $n_s = 20$  SPM,  $\phi = 60$ ,  $L_p = 0.254$  m,  $r_p = 0.00635$  m).

In the Karakas-Tariq method, it is assumed that the perforations have a cylindrical shape surrounded by an isotropic crushed zone. External boundary of the crushed zone is assumed to be cylindrical, too. However, the proposed model can be used for any perforated completions as long as the helical symmetry can be established around the wellbore.



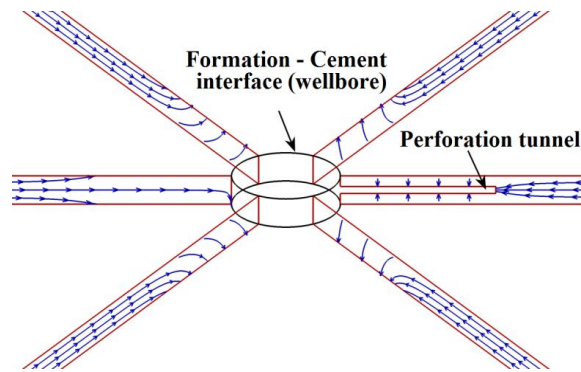


Figure 17. Typical streamline pattern on vertical planes crossing the axis of perforations ( $n_s = 20$  SPM,  $\phi = 60$ ,  $L_p = 0.254$  m,  $r_p = 0.00635$  m)

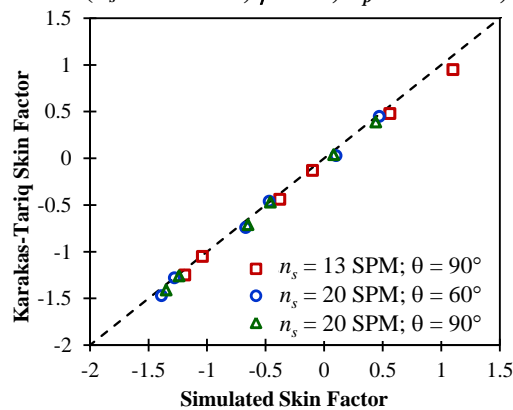


Figure 18. Skin factor comparison between the proposed model and the semi-analytical method

## Conclusion

In this study, repetitive patterns of the flow into cased-and-perforated vertical wells are examined and available models for reproducing this pattern are categorized into two groups of OCM and HPM. A new model based on the finite element method and helical symmetry of the flow pattern was suggested. The proposed model just

requires a horizontal section of the formation containing one perforation tunnel to be explicitly simulated.

Enforcement of the periodic boundary conditions to the representative formation in order to ensure compatibility of the pressure and correct computation of the velocity is discussed. With respect to the ambiguity in imposing velocity-periodic part, using weighted integral formulation, proved that for problems with repetitive symmetry, this part of the boundary conditions is satisfied automatically.

The accuracy of the proposed model was demonstrated through comparison by the middle perforated layer in a formation with three cycles of perforations. The efficiency of the proposed model was examined through comparison by one-cycle and half-cycle models. The proposed model has more simple boundary conditions compared to HPM and is more efficient than OCM. It divides the efforts required to conduct a numerical simulation (preprocessing) and solution of equations, into more manageable portions and can easily be used to simulate flow into perforated completions.

Application of the model to estimate the skin factor for perforated completions was discussed through comparing with the common semi-analytical method. The semi-analytical method for skin factor calculation requires that the geometry of the perforation tunnels and their crushed zones be cylindrical. Moreover, anisotropy of the crushed zone cannot be accounted for by this method. However, the proposed model can be used for any perforated completions as long as

the geometry, material properties, and the boundary conditions of the global system have helically repetitive pattern around the wellbore.

### References

1. Zhan L., Doornbosch F., Martin A., Harvey J., Brenden G., "Perforated Completion Optimization Using a New, Enhanced and Integrated Perforating Job Design Tool," Presented at the SPE International Symposium and Exhibition on Formation Damage Control, Lafayette, Louisiana, USA, (2012).
2. Hagoort J., "An analytical model for predicting the productivity of perforated wells", *J Petrol Sci Eng.* vol. 56 (2007) 199-218.
3. Hashemi S. M., Zamani E., Mahdian A., "Numerical simulation and performance optimization of oil well perforator", *Modares Mechanical Engineering*, vol. 16, no. 3, (2016) 17-26 (in Persian)
4. Satti R., Betancourt D., Harvey W, Zuklic S, White R, Ochsner D, Sampson T, Myers W, Gilliat J, "Beginning with the End in Mind: Shaped Charges Designed for Reservoir Conditions", Presented at the SPE Middle East Oil & Gas Show and Conference, Manama, Kingdom of Bahrain (2017).
5. Karakas M., Tariq S. M., "Semianalytical Productivity Models for Perforated Completions", *SPE Production Engineering.* vol. 6, no. 1, (1991) 73-82.
6. Bellarby J., "Well completion design", *Developments in Petroleum Science*, vol. 56, Elsevier, Hungary (2009).
7. Harris M. H., "The effect of perforating on well productivity," *J Petrol Technol*, vol. 18 (1966) 518-528.

8. Klotz J. A., Krueger F. F., Pye D. S., "Effect of perforating damage on well productivity", *J Petrol Technol*, vol. 29, no. 2, (1974) 1303-1314.
9. Locke S., "An Advanced Method for Predicting the Productivity Ratio of a Perforated Well", *J Petrol Technol*, vol. 33, (1981) 2481-2488.
10. Dogulu Y. S., "Modeling of Well Productivity in Perforated Completions", Presented at the SPE Eastern Regional Meeting, Pittsburgh, Pennsylvania, USA, (1998).
11. Ansah J., Proett M. A., Soliman M. Y., "Advances in Well Completion Design: A New 3D Finite-Element Wellbore Inflow Model for Optimizing Performance of Perforated Completions", Presented at the SPE International Symposium and Exhibition on Formation Damage Control, Lafayette, Louisiana (2002).
12. Jamiolahmady M., Danesh A., Sohrabi M., Ataei R., "Gas condensate flow in perforated region", *SPE Journal*, vol. 12, no. 1, (2007) 89-99.
13. Byrne M., Jimenez M. A., Chavez J. C., "Predicting Well Inflow Using Computational Fluid Dynamics-Closer to the Truth?", Presented at the SPE European Formation Damage Conference, Scheveningen, The Netherlands, (2009).
14. Sun D., Li B., Gladkikh M., Satti R., Evans R., "Comparison of Skin Factors for Perforated Completions Calculated with Computational-Fluid-Dynamics Software and the Karakas-Tariq Semianalytical Model", *SPE Drilling & Completion*, vol. 28, no. 1, (2013) 21-33.
15. Volonte G., Scarfato F., Brignoli M., "sand prediction: a practical finite-element 3d approach for real field applications," *SPE Production & Operations*, vol. 28, no. 1, (2013) 95-108.
16. Wang H., Cardiff P., Sharma M. M., "A 3-d poro-elasto-plastic model for sand production around open-hole and cased & perforated wellbores,"

Presented at the 50th US Rock Mechanics / Geomechanics Symposium, Houston, Texas, USA, (2016).

17. Segal G., Vuik K., Kassels K., "On the implementation of symmetric and antisymmetric periodic boundary conditions for incompressible flow," *Int. J. Numer. Meth. Fluids.* vol. 18, (1994) 1153-1165.
18. Li S. "On the nature of periodic traction boundary condition in micromechanical FE analyses of unit cells", *IMA J. Appl. Math.*, vol. 77, (2012) 441-450.
19. Yildiz T., "Productivity of Selectively Perforated Vertical Wells", Presented at the SPE International Oil and Gas Conference and Exhibition in China, Beijing, China, (2000).
20. Xia Z., Zhang Y., Ellyin F., "A unified periodical boundary conditions for representative volume elements of composites and applications", *Int J Solids Struct.*, vol. 40, (2003) 1907-1921.
21. Tyrus J. M., Gosz M., DeSantiago E., "A local finite element implementation for imposing periodic boundary conditions on composite micromechanical models", *Int J Solids Struct.*, vol. 44, (2007) 2972-2989.
22. Reddy J. N., "An Introduction to the Finite Element Method", 3<sup>rd</sup> ed., Singapore. McGraw-Hill. (2006).
23. Zienkiewicz O. C., Taylor R. L., Zhu J. Z., "The Finite Element Method: Its Basis and Fundamentals", 7<sup>th</sup> ed, UK, Elsevier Butterworth-Heinemann (2013).
24. Nguyen V.D., Bechet E., Geuzaine L., Noels L., "Imposing periodic boundary condition on arbitrary meshes by polynomial interpolation", *Electrical Engineering*, vol. 55, (2011) 390-409.

25. Sandstom C., Larsson F., Runesson K., "Weakly periodic boundary conditions for the homogenization of flow in porous media", *Adv Model Simul Eng Sci.*, vol. 2, no. 12, (2014) 1-24.
26. Brooks J.E., "A Simple Method for Estimating Well Productivity", Presented at the SPE European Formation Damage Conference, The Hague, The Netherlands, (1997).
27. Yildiz T., "Assessment of Total Skin Factor in Perforated Wells", *SPE Reservoir Evaluation & Engineering*, vol. 9. no. 1, (2006) 62-76.
28. Jamiolahmady M., Mahdiyar H., Ghahri P., Sohrabi M., "A new method for productivity calculation of perforated wells in Gas condensate reservoirs", *J Petrol Sci Eng*, vol. 77, (2011) 263-273.
29. Dake L. P., "Fundamentals of Reservoir Engineering", Elsevier Science, Netherlands (1983).